ACS EARTH AND SPACE CHEMISTRY

Article

Cite This: ACS Earth Space Chem. 2019, 3, 1189−1195

http://pubs.acs.org/journal/aesccq

Astronomical Search of Vinyl Alcohol Assisted by Submillimeter Spectroscopy

Mattia Melosso,*[,†] Brett A. McGuire,[‡,§] Filippo Tamassia,[∥] Claudio Degli Esposti,[†] and Luca Dore*[,†]

[†]Dipartimento di Chimica "Giacomo Ciamician", Università di Bologna, Via Francesco Selmi 2, 40126 Bologna, Italy

[‡]National Radio Astronomy Observatory, Charlottesville, Virginia 22903, United States

[§]Harvard−Smithsonian Center for Astrophysics, Cambridge, Massachusetts 02138, United States

[∥]Dipartimento di Chimica Industriale "Toso Montanari", Università di Bologna, Viale del Risorgimento 4, 40136 Bologna, Italy

Supporting Information

ABSTRACT: We report an extension toward the submillimeter domain of the laboratory spectroscopy of the *syn* and *anti* conformers of vinyl alcohol, a species that has been detected once in the interstellar medium, in the massive star-forming region Sagittarius B2(N) (Turner, B. E.; Apponi, A. Microwave detection of interstellar vinyl alcohol, CH_2CHOH. *Astrophys. J.* **2001**, *561*, L207−L210, 10.1086/324762). Spectra were recorded with high accuracy (15−20 kHz) between 245 and 310 GHz by a frequency-modulation spectrometer equipped with a pyrolysis cell. Using these spectra and the refined molecular constants, we have searched for vinyl alcohol in the publicly available spectral line surveys from the ASAI [Astrochemical Surveys at Institut de Radioastronomie Millimétrique (IRAM)] Large Project, whose source sample spans the evolutionary range of a solar-type protostar and covering 75−350 GHz (4−1 mm) in frequency. We report non-detections in all nine sources, derive upper limits to the abundance of both conformers of vinyl alcohol, and comment on possible chemical and physical explanations for the non-detections.

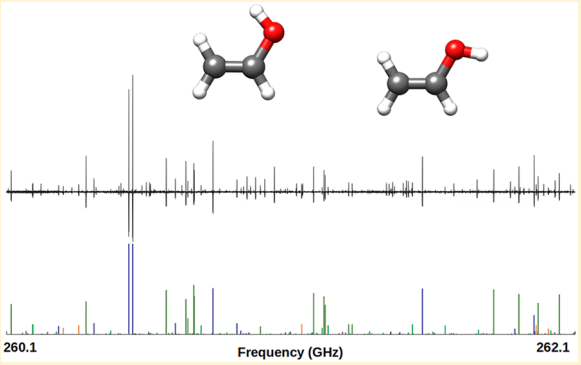

KEYWORDS: *vinyl alcohol, complex organic molecules, star-forming regions, spectroscopy, ISM, pyrolysis*

1. INTRODUCTION

Vinyl alcohol (VA, CH_2═CH−OH) is the simplest enol, with a hydroxy group (−OH) bonded to a vinyl group (−CH═CH_2). VA can exist in two rotameric forms, depending upon the value of the C═C−O−H dihedral angle ϕ: for the *syn* conformer, $\phi = 0°$ and the hydrogen of the hydroxy group is in the plane of the molecule on the side of the double bond, whereas in the *anti* case, there is a torsion of 180° of the hydroxy group. The interconversion between the two forms is hindered by an energy barrier of 21 kJ/mol,[1] with the *syn* rotamer lower in energy than the *anti* rotamer by 4.6 kJ/mol.[2] The conversion of *syn*-VA to acetaldehyde (CH_3CHO) is an example of keto−enol tautomerism; the reaction is exothermic by 40.5 kJ/mol,[2] making acetaldehyde much more thermodynamically stable. However, a high energy barrier makes the thermal unimolecular conversion very unlikely.[3] Along with oxirane [$(CH_2CH_2)O$, also known as cyclic ethylene oxide], these complex organic molecules (COMs) form the three-membered isomeric family (C_2, H_4, and O). Their relative stabilities are[4] acetaldehyde (0 kJ/mol), *syn*-VA (40.5 kJ/mol), *anti*-VA (45.1 kJ/mol), and oxirane (115.5 kJ/mol).

Detections of all of these species have been reported in the interstellar medium (ISM).[5] Acetaldehyde is ubiquitous in the ISM: it has been detected in cold dust clouds, prestellar cores, cold envelopes, hot cores and corinos, and protostellar shocks (see the study by Codella et al.[6] and references therein). Oxirane has been found in a variety of interstellar environments, and where it has been observed, acetaldehyde is always present. Since the first reported detection in Sgr B2(N),[7] oxirane has been observed in hot cores,[8] massive star-forming regions,[9] and the Galactic Center.[10] VA, on the other hand, has only been detected toward Sgr B2(N),[11] driving questions of its formation chemistry and efficiency relative to its two more widespread isomers. Turner and Apponi[11] proposed a gas-phase reaction of CH_3^+ with formaldehyde (H_2CO) to form VA, but Charnley[12] ruled out the possibility that any C_2H_4O isomer could be formed via ion−molecule reactions, which would require unrealistically high abundances of the precursor species. Solid-state formation on dust grains via radiation-induced processes in ice mantles, followed by desorption into the gas phase, appears more likely.[13] This formation route has

Special Issue: Complex Organic Molecules (COMs) in Star-Forming Regions

Received: March 14, 2019
Revised: May 31, 2019
Accepted: June 3, 2019
Published: June 3, 2019

DOI: 10.1021/acsearthspacechem.9b00055
ACS Earth Space Chem. 2019, 3, 1189−1195

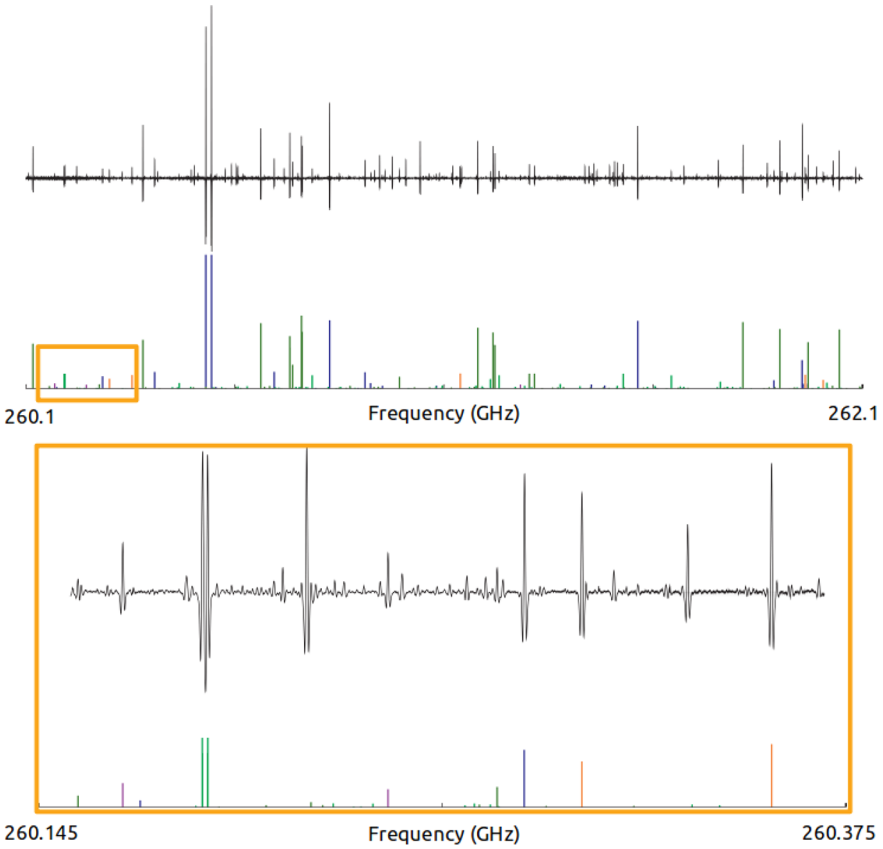

Figure 1. (Upper panel) 2 GHz portion of the millimeter wave spectrum recorded in this work. The black trace is the experimental spectrum, while colored sticks mark simulated transitions of ethylene glycol (green), acetaldehyde (blue), and VA (orange and purple for *syn* and *anti*, respectively). The spectrum was simulated assuming a temperature of 300 K and an abundance ratio of 1:0.8:0.5:0.05 between acetaldehyde, ethylene glycol, *syn*-VA, and *anti*-VA, respectively. (Lower panel) Portion of the spectrum enlarged to show detail.

been studied in the laboratory by Hudson and Moore,[14] who irradiated ices of water (H_2O) and acetylene (C_2H_2) at 15 K with protons and ultraviolet (UV) photons and observed the production of VA. Bennett et al.[13] bombarded a mixture of carbon dioxide (CO_2) and ethylene (C_2H_4) with electrons and identified all of the C_2H_4O isomers as products of the addition of oxygen atoms to ethylene, although VA was the minor product. In a separate study, Ward and Price[15] investigated the reactions of ethylene and propylene ($CH_3CH{=}CH_2$) with thermalized oxygen atoms at 12−90 K but did not observe the formation of VA, whereas the major product was oxirane. These experimental observations are therefore consistent with the fact that, in the isomeric family (C_2, H_4, and O), VA appears to be the least abundant and least often detected species in the ISM. That said, the number of reported observational attempts to identify and quantify VA in the ISM, even to obtain upper limits to constrain chemical models, is limited.

The laboratory spectroscopic characterization of gas-phase VA dates back to 1976, when Saito[16] identified the *syn* conformer by its microwave (MW) spectrum in the products of the thermal dehydration of ethylene glycol [$(CH_2OH)_2$]. Both *a*-type [μ_a = 0.616(7) D] and *b*-type [μ_b = 0.807(6) D] rotational transitions were observed for the parent and $CH_2{=}$CH−OD isotopologues, strongly supporting a planar structure for *syn*-VA that was later confirmed by a comprehensive study of nine isotopologues.[17] Some years later, Rodler[18] recorded the MW spectrum of *anti*-VA, which has a larger dipole moment [μ_a = 0.547(2) D, and μ_b = 1.702(1) D] but higher energy (ΔE = 4.6 kJ/mol) than *syn*-VA.

Recently, Hays et al.[19] recorded the spectrum of the *syn* conformer in the frequency range of 142−446 GHz. However, because of the limited sampling of rotational energy levels ($1 \leq J \leq 10$, and $0 \leq K_a \leq 4$), the centrifugal distortion analysis was limited to the quartic terms. As for the *anti* conformer, far-infrared (FIR) measurements of the ν_{15} band[20] (OH torsional fundamental) led to a refinement of the ground state constants, with the determination of two sextic centrifugal distortion terms.

In this study, we report the extension of the laboratory spectroscopy of the vibrational ground state of both conformers of VA to include the 245−310 GHz range. An accurate centrifugal distortion analysis up to the sixth order allowed us to obtain rotational and distortion constants for both rotamers. Using these constants, rest frequencies for a wide range of J and K_a quantum numbers can now be derived with confidence to high precision. On the basis of these new predictions, we have searched the ASAI [Astronomical Surveys at Institut de Radioastronomie Millimétrique (IRAM)] unbiased high-sensitive spectral surveys at millimeter and submillimeter wavelengths (75−350 GHz) for both conformers.

2. EXPERIMENTAL DETAILS

Because VA is a metastable molecule that readily converts to the more stable acetaldehyde, it has to be produced *in situ*. In this work, VA was generated through flash vacuum pyrolysis of

DOI: 10.1021/acsearthspacechem.9b00055
ACS Earth Space Chem. 2019, 3, 1189−1195

Table 1. Spectroscopic Constants of *syn*- and *anti*-VA[a]

		syn-VA			*anti*-VA		
constant		this work	CDMS	Hays et al.[19]	this work	CDMS	Bunn et al.[20]
A		59660.76998(86)	59660.774(11)	59660.7824(30)	62868.0926(13)	62868.092(11)	62868.0949(91)
B		10561.60623(23)	10561.6054(19)	10561.60521(74)	10455.74661(37)	10455.7472(19)	10455.7461(15)
C		8965.84199(21)	8965.8421(17)	8965.84204(66)	8963.32039(34)	8963.3210(17)	8963.3210(14)
D_J	$\times 10^3$	7.51689(54)	7.490(15)	7.4975(41)	7.08257(96)	7.095(17)	7.0732(29)
D_{JK}		−0.0597550(47)	−0.06000(25)	−0.059876(56)	−0.0571690(79)	−0.05698(32)	−0.057423(86)
D_K		0.914229(19)	0.91405(75)	0.91485(19)	1.123638(43)	1.1228(12)	1.12509(42)
d_1	$\times 10^3$	−1.66888(13)	−1.6653(12)	−1.66572(44)	−1.49725(17)	−1.4968(13)	−1.49475(32)
d_2	$\times 10^3$	−0.116210(66)	−0.11579(14)	−0.11578(10)	−0.109426(83)	−0.10933(24)	−0.108858(73)
H_J	$\times 10^9$	9.75(44)			7.30(86)		
H_{JK}	$\times 10^6$	−0.1096(66)			−0.1901(96)	−0.58(111)	−0.881(72)
H_{KJ}	$\times 10^6$	−4.291(18)			−4.354(48)		
H_K	$\times 10^3$	0.04388(20)	−0.0297(79)		0.05397(56)		0.0528(18)
h_1	$\times 10^9$	4.60(19)			3.69(22)		
h_2	$\times 10^9$	0.77(16)			1.05(18)		
h_3	$\times 10^9$	0.192(46)			0.114(57)		
number of data		242			132 (+1335 FIR)		
RMS error		0.039			0.018		
σ		0.92			0.91		

[a]Parameter standard errors are reported in parentheses in units of the last quoted digit. All units are in MHz with the exception of σ (dimensionless).

gaseous ethylene glycol at ca. 1400 K. The same apparatus has successfully been used for the production of other COMs [*C*-cyanomethanimine (NCCH=NH)[21] and ethanimine (CH_3CH=NH)[22]]. The experimental setup is described in detail in those works.

The rotational spectra of both *syn* and *anti* conformers of VA were recorded with a frequency-modulation millimeter spectrometer described in detail elsewhere.[23] Briefly, for this work, a Gunn diode (Radiometer Physics GmbH, J.E. Carlstrom Co.) emitting in the 80−115 GHz range was coupled with a passive frequency tripler (WR3.4X2, Virginia Diodes) providing spectral coverage between 245 and 310 GHz. The frequency stability was ensured by locking the Gunn diode, via a phase-lock loop, to a harmonic of a radio frequency (RF) local oscillator (LO), which was referenced to a 5 MHz rubidium frequency standard. The frequency modulation of the radiation was obtained by a sine wave modulating, at f = 48 kHz, the 75 MHz reference signal (IF). The output signal was detected by a zero-biased, Schottky diode detector (WR3.4ZBD, Virginia Diodes) and demodulated at 2f by a lock-in amplifier.

3. ANALYSIS OF THE SPECTRUM

The rotational spectrum of VA has been previously investigated at low frequency, up to 56 and 126 GHz for the *anti*[18] and *syn*[16,24,25] conformers, respectively. Line catalogs based on these works are present in the Cologne Database for Molecular Spectroscopy (CDMS).[26] In addition, a set of refined spectroscopic constants is available from Hays et al.[19] for *syn*-VA. Using the available parameters and dipole moment components from Saito,[16] the spectra of *syn*- and *anti*-VA were predicted at millimeter and submillimeter frequencies using the SPFIT/SPCAT suite of programs.[27]

The observed spectrum was dominated by transitions belonging to the pyrolitic precursor ethylene glycol and acetaldehyde (formed during the pyrolysis). Nevertheless, the line assignment for VA was straightforward as a result of the efficient production of VA in the quartz reactor and the sensitivity of our spectrometer, resulting in a spectrum with high S/N (see Figure 1).

Ground-state rotational transitions of both conformers were recorded in the frequency region of 245−310 GHz and involve energy levels with J values spanning from 2 to 38 and K_a values from 0 to 13. For each conformer, the newly observed transition frequencies, along with data previously reported,[16,18−20,25] have been analyzed using a standard semi-rigid Watson *S*-reduced Hamiltonian,[28] suitable for a nearly prolate asymmetric rotor, such as VA. For the purpose of this work, centrifugal distortion terms up to the sextic power of the rotational angular momentum were used.

The analysis included 242 and 135 pure rotational transition frequencies for *syn*- and *anti*-VA, respectively. The rovibrational transitions measured by Bunn et al.[20] were also included in the analysis of the *anti* conformer: they involve energy levels with values of J as high as 59 and K_a in the range of 0−16. In the least squares procedure, each datum was weighted according to its uncertainty. For frequencies obtained from the literature, the uncertainties quoted in the CDMS have been retained (20−70 kHz) and the uncertainty of the FIR data was set to their reported error of 2.4×10^{-4} cm^{-1}. We believe that the uncertainties in the transition frequencies reported by Hays et al.[19] were underestimated. The standard deviation of their fit, which also includes previous measurements,[16,25] is 1.4; this can be reduced to ∼1 by just doubling the uncertainties of Hays et al.[19] Thus, for this work, we assumed these uncertainties to be 40 kHz below 220 GHz and 80 kHz above 220 GHz. The accuracy of our measurements is assumed to be 15−20 kHz. A few lines, whose residual exceeded 3 times this experimental error, were discarded at the end of the fitting procedure.

The fits were carried out using the SPFIT/SPCAT suite of programs.[27] The resulting fits had standard deviations (σ) slightly lower than 1 for each isomer, indicating that the model appropriately reproduces the observed data within the uncertainties. The fits include enlarged and refined sets of spectroscopic parameters. Particularly, the precision of the

DOI: 10.1021/acsearthspacechem.9b00055
ACS Earth Space Chem. 2019, 3, 1189−1195

Table 2. 1σ Upper Limits to the Column Density of *syn*- and *anti*-VA in Each Source and Transition and Pertinent Parameters Used for the Calculation

source	transition $J'_{K_a,K_c}-J''_{K_a,K_c}$	frequency[a] (MHz)	ΔV (km s^{-1})	T_{ex} (K)	E_u (K)	$S_{ij}\mu^2$ (Debye^2)	ΔT_{A^*}[b] (K)	Q_r	N_T (cm^{-2})	X_{H_2}	reference[c] (N_T/T_{ex})
					syn-VA						
B1	$3_{1,3}-2_{0,2}$	103706.0(1)	0.8	10	7.878	1.299	2.9	72	$\leq 6\times10^{11}$	$\leq 4\times10^{-12}$	21 and 36
IRAS4A	$5_{0,5}-4_{0,4}$	96874.91(2)	5.0	21	13.994	1.8743	2.6	217	$\leq 5\times10^{12}$	$\leq 5\times10^{-12}$	31 and 21
L1157-B1	$12_{1,12}-11_{0,11}$	238773.681(3)	8.0	60	72.127	5.6505	2.9	1045	$\leq 1\times10^{13}$	$\leq 1\times10^{-8}$	32
L1157mm	$13_{1,13}-12_{0,12}$	254003.32(2)	8.0	60	83.683	6.2875	4.1	1045	$\leq 1\times10^{13}$	$\leq 1\times10^{-8}$	32
L1448-R2	$11_{0,11}-10_{0,10}$	207668.69(2)	8.0	60	60.667	4.1097	4.7	1045	$\leq 2\times10^{13}$	$\leq 6\times10^{-11}$	*d* and 37
L1527	$3_{1,3}-2_{0,2}$	103706.0(1)	0.5	12	7.878	1.299	1.9	94	$\leq 3\times10^{11}$	$\leq 1\times10^{-11}$	33 and 37
L1544	$3_{1,3}-2_{0,2}$	103706.0(1)	0.5	10	7.878	1.299	4.4	72	$\leq 5\times10^{11}$	$\leq 5\times10^{-12}$	34 and 38
SVS13A	$3_{1,3}-2_{0,2}$	103706.0(1)	3.0	19	7.878	1.299	2.0	187	$\leq 2\times10^{12}$	$\leq 2\times10^{-12}$	31 and 21
TMC1	$5_{1,5}-4_{0,4}$	135877.21(2)	0.3	7	15.866	2.0245	9.6	42	$\leq 9\times10^{11}$	$\leq 6\times10^{-11}$	35 and 39
					anti-VA						
B1	$2_{1,2}-1_{0,1}$	89757.10(3)	0.8	10	5.24	4.3058	2.6	70	$\leq 2\times10^{11}$	$\leq 1\times10^{-12}$	21 and 36
IRAS4A	$7_{0,7}-6_{1,6}$	94992.77(5)	5.0	21	25.909	10.7237	2.5	213	$\leq 2\times10^{12}$	$\leq 2\times10^{-12}$	31 and 21
L1157-B1	$9_{1,8}-9_{0,9}$	94064.95(5)	8.0	60	45.975	19.3221	1.7	1024	$\leq 3\times10^{12}$	$\leq 3\times10^{-9}$	32
L1157mm	$9_{1,8}-9_{0,9}$	94064.95(5)	8.0	60	45.975	19.3221	2.8	1024	$\leq 5\times10^{12}$	$\leq 4\times10^{-9}$	32
L1448-R2	$9_{1,8}-9_{0,9}$	94064.95(5)	8.0	60	45.975	19.3221	2.7	1024	$\leq 5\times10^{12}$	$\leq 1\times10^{-11}$	*d* and 37
L1527	$3_{1,3}-2_{0,2}$	106949.48(3)	0.5	12	7.928	5.7826	2.9	92	$\leq 8\times10^{10}$	$\leq 3\times10^{-12}$	33 and 37
L1544	$2_{1,2}-1_{0,1}$	89757.10(3)	0.5	10	5.24	4.3058	2.5	70	$\leq 7\times10^{10}$	$\leq 7\times10^{-13}$	34 and 38
SVS13A	$3_{1,3}-2_{0,2}$	106949.48(3)	3.0	19	7.928	5.7826	2.8	183	$\leq 7\times10^{11}$	$\leq 7\times10^{-13}$	31 and 21
TMC1	$5_{1,5}-4_{0,4}$	139315.20(4)	0.3	7	15.984	8.9726	6.8	42	$\leq 1\times10^{11}$	$\leq 2\times10^{-11}$	35 and 39

[a]Uncertainties are given in units of the last significant digit. The full experimental linelist with references is provided as Supporting Information, including uncertainties. [b]Taken as the RMS noise level of the observations in the region of the indicated transition. [c]Reference from which an average value of ΔV and T_{ex} was obtained for the source. [d]For this shocked location within a molecular outflow, the same parameters were assumed as for L1157-B1.

rotational constants *A*, *B*, and *C* has been improved by ∼30% for *syn*-VA and ∼25% for *anti*-VA (only 14% for *A*); the error associated with the quartic centrifugal distortion terms has been remarkably reduced, in some cases by up to 1 order of magnitude; and sextic centrifugal distortion parameters were determined for the first time (see Table 1). These new sets of constants have better predictive capability within the investigated frequency range and are likely reliable for accurate predictions of transitions with *J* up to ∼40 for *syn*-VA and ∼60 for *anti*-VA and relatively low K_a values. Finally, these sets of constants constitute a solid base for future investigations at even higher frequencies.

4. ASTRONOMICAL SEARCH

We have searched for both *syn*- and *anti*-VA in the publicly available spectra from the ASAI Large Project (http://www.oan.es/asai/). Full details of the observations, data reduction, and sources are provided by Lefloch et al.,[29] and are only briefly summarized here. The source sample spans the evolutionary range of a solar-type protostar from the precore, dark cloud stage (e.g., TMC-1) to class 0/I protostars, including locations at the shocked regions of outflows from these source (e.g., L1157-B1). Line surveys were carried out with the broad-band eight mixer receiver (EMIR) at the IRAM 30 m telescope. The spectral coverage varied from source to source, with a number of the warmer sources spanning from ca. 4 to 1 mm (75−350 GHz). Typical root-mean-square (RMS) noise values were as low as ∼2 mK at 3 mm in many sources and up to ∼5−10 mK, particularly at higher frequencies. Spectral resolution was sufficient in all cases to provide at least three points across the expected linewidths for each source.

Column density upper limits were calculated assuming a single-excitation temperature model following the formalisms of Hollis et al.[30] using eq 1 below

$$N_T = \frac{1}{2}\frac{3k}{8\pi^3}\sqrt{\frac{\pi}{\ln 2}}\frac{Q\,e^{E_u/T_{ex}}\Delta T_b \Delta V}{B\nu S_{ij}\mu^2}\frac{1}{1-\frac{e^{h\nu/kT_{ex}}-1}{e^{h\nu/kT_{bg}}-1}} \quad (1)$$

where N_T is the total column density (cm^{-2}), Q is the partition function, T_{ex} is the excitation temperature (K), E_u is the upper state energy (K), ΔT_b is the peak intensity (K), ΔV is the full width at half maximum of the line (km s^{-1}), B is the beam filling factor, ν is the frequency (Hz), S_{ij} is the intrinsic quantum mechanical line strength, μ is the permanent dipole moment [Debye (care must be taken to convert this unit for compatibility with the rest of the parameters)], and T_{bg} is the background continuum temperature (K). For this analysis, the source was assumed to fill the beam in each case (B = 1). The background temperature was set to 2.7 K; we expect this to introduce trivial uncertainty in the derived upper limits (<10%). The partition function was taken to be dominated by the rotational partition function, with no contribution from low-lying vibrational states, given the low temperatures assumed.

For the upper limits presented here, a simulated spectrum was generated using the parameters described for each observation in Table 2. Source-specific parameters (line width, excitation temperature, and H_2 column density) were obtained from the indicated references; ΔV and T_{ex} were chosen to be representative of other complex molecules in the source. Many of these sources have been shown by high-resolution interferometric observations to contain an underlying substructure, which is unresolved in the IRAM beam, which varies from 25″ to 8″ between 3 and 1 mm (see

DOI: 10.1021/acsearthspacechem.9b00055
ACS Earth Space Chem. 2019, 3, 1189−1195

references in Table 2). Rather than assume a source size for VA based on an implied chemical relation to other species in these regions, we calculate a beam-averaged upper limit. If the underlying source is more compact, a more stringent upper limit could be placed, making our values at worst overly conservative.

The transition of *syn*- or *anti*-VA used to calculate the 1σ upper limit in each source was chosen based on the ratio of the strength of the line to the noise level of the observations. The upper limit was then calculated by taking the RMS noise value measured in that region as the peak line intensity. The chosen lines and resulting upper limits are given in Table 2. In many cases, the lines that were used to calculate the upper limits are at the lowest frequencies of the observations and are indeed within the range of previous laboratory measurements. This is due to the increasing noise in the observations at the higher frequencies now accessible with the laboratory work described here. More sensitive observations at 2 and 1 mm (>200 GHz) would enable the use of our laboratory results to derive more stringent constraints and even enable a new interstellar detection.

5. DISCUSSION

The first and, to our knowledge, only claimed detection of either conformer of VA in the ISM was reported by Turner and Apponi[11] in Kitt Peak 12 m telescope observations of Sgr B2(N) between 1 and 2 mm. The detection was based on the existing laboratory work at the time, which covered up to ∼126 GHz (*syn* conformer)[16] and 56 GHz (*anti* conformer).[18] Turner and Apponi[11] claimed a detection of two lines of *syn*-VA and five lines of *anti*-VA and derived column densities in Sgr B2(N) of 2.0×10^{14} and 2.4×10^{13} cm^{-2}, respectively. Assuming[40] a column density of H_2 of 10^{24} cm^{-2}, these yield abundances of $X_{H_2} = 2.0 \times 10^{-10}$ and 2.4×10^{-11} for *syn*- and *anti*-VA, respectively. A subsequent observational search for both conformers in Sgr B2(N) could not confirm the detection but stopped short of refuting the identification outright, suggesting that their observations were not particularly sensitive to a potentially spatially extended population of VA.[41]

The abundances established by Turner and Apponi[11] are higher than all of our established upper limits, except for those in L1157mm and L1157-B1. The sources observed here are all at a much earlier evolutionary stage than Sgr B2(N). This may suggest that VA is primarily formed in the solid phase on the icy surfaces of dust grains and is not ejected into the gas phase until the source has progressed past the protostellar phase and injected sufficient energy into the system to thermally liberate the molecules from the grains. The lack of a detection, at lower abundance ratios than in Sgr B2(N), in the L1448 shock front, however, casts a small doubt on this scenario. In principle, the shock front of a molecular outflow should result in the bulk, non-thermal liberation of complex molecules into the gas phase, allowing for their detection before temperatures are high enough for thermal desorption.[42,43] Our analysis may indicate that VA was not present in these ices at the time of their desorption in the shock. Alternatively, it is possible that the high-temperature, high-pressure conditions immediately following the shock resulted in the rapid destruction of any detectable population of VA.

6. CONCLUSION

The high-resolution rotational spectrum of the *syn* and *anti* conformers of VA has been recorded between 245 and 310 GHz by submillimeter wave spectroscopy. Newly observed transitions with J and K_a values as high as 38 and 13, respectively, have been measured and analyzed in a global fit, which included the available literature data. The precision of the rotational and quartic centrifugal distortion constants has been substantially improved by these new measurements. Moreover, sextic centrifugal distortion terms could be determined for the first time for both conformers. This is particularly important if higher frequency transitions need to be predicted to guide future laboratory studies and astronomical searches in warmer sources. Indeed, at any temperature above 50 K, the strongest transitions of the spectrum of VA fall above 600 GHz. In this respect, further investigation of the laboratory spectrum of VA at higher frequencies (up to the terahertz region) might be useful in combination with Atacama Large Millimeter/submillimeter Array (ALMA) observations, which offer high sensitivity and high spectral and spatial resolution.

We have searched for both conformers in the publicly available spectra from the ASAI Large Project, which includes observations of several different evolutionary stages of a solar-type protostar, i.e., from starless cores to class 0 and I objects, and in addition shocked regions. We report non-detections in all sources and derive upper limits to the column densities of *syn*- and *anti*-VA in each source. The detection of VA exclusively in Sgr B2(N) may suggest that this species is primarily formed on the icy surfaces of dust grains and then thermally released into the gas phase. However, the lack of detection in the L1448 shock front casts some doubt on this theory. More astronomical searches, astrochemical models, and laboratory data are therefore necessary to derive a solid theory about the formation of interstellar VA.

■ ASSOCIATED CONTENT

Supporting Information

The Supporting Information is available free of charge on the ACS Publications website at DOI: 10.1021/acsearthspacechem.9b00055.

Observed transitions, containing measured rotational transitions and residuals from the fit for the two conformers of VA (TXT)

■ AUTHOR INFORMATION

Corresponding Authors

*E-mail: mattia.melosso2@unibo.it.

*E-mail: luca.dore@unibo.it.

ORCID

Luca Dore: 0000-0002-1009-7286

Notes

The authors declare no competing financial interest.

■ ACKNOWLEDGMENTS

This study was supported by Bologna University (RFO funds) and the Ministry of Education, Universities and Research (MIUR, Project PRIN 2015: STARS in the CAOS, Grant 2015F59J3R). The National Radio Astronomy Observatory is a facility of the National Science Foundation operated under cooperative agreement by Associated Universities, Inc. The

DOI: 10.1021/acsearthspacechem.9b00055
ACS Earth Space Chem. 2019, 3, 1189−1195

Green Bank Observatory is a facility of the National Science Foundation operated under cooperative agreement by Associated Universities, Inc. Support for Brett A. McGuire was provided by the National Aeronautics and Space Administration (NASA) through Hubble Fellowship Grant HST-HF2-51396 awarded by the Space Telescope Science Institute, which is operated by the Association of Universities for Research in Astronomy, Inc., for NASA, under Contract NAS5-26555.

REFERENCES

(1) Bunn, H.; Hudson, R. J.; Gentleman, A. S.; Raston, P. L. Far-infrared synchrotron spectroscopy and torsional analysis of the important interstellar molecule, vinyl alcohol. *ACS Earth Space Chem.* **2017**, *1*, 70−79.

(2) Estep, M. L.; Morgan, W. J.; Winkles, A. T.; Abbott, A. S.; Villegas-Escobar, N.; Mullinax, J. W.; Turner, W. E.; Wang, X.; Turney, J. M.; Schaefer, H. F. Radicals derived from acetaldehyde and vinyl alcohol. *Phys. Chem. Chem. Phys.* **2017**, *19*, 27275−27287.

(3) Snyder, J. W., Jr.; Mazziotti, D. A. Photoexcited tautomerization of vinyl alcohol to acetylaldehyde via a conical intersection from contracted Schröedinger theory. *Phys. Chem. Chem. Phys.* **2012**, *14*, 1660−1667.

(4) Martin-Drumel, M.-A.; Lee, K. L. K.; Belloche, A.; Zingsheim, O.; Thorwirth, S.; Müller, H. S.; Lewen, F.; Garrod, R. T.; Menten, K. M.; McCarthy, M. C.; Schlemmer, S. Submillimeter spectroscopy and astronomical searches of vinyl mercaptan, C_2H_3SH. *Astron. Astrophys.* **2019**, *623*, A167.

(5) McGuire, B. A. 2018 census of interstellar, circumstellar, extragalactic, protoplanetary disk, and exoplanetary molecules. *Astrophys. J., Suppl. Ser.* **2018**, *239*, 17.

(6) Codella, C.; Fontani, F.; Ceccarelli, C.; Podio, L.; Viti, S.; Bachiller, R.; Benedettini, M.; Lefloch, B. Astrochemistry at work in the L1157-B1 shock: Acetaldehyde formation. *Mon. Not. R. Astron. Soc.: Lett.* **2015**, *449*, L11−L15.

(7) Dickens, J. E.; Irvine, W. M.; Ohishi, M.; Ikeda, M.; Ishikawa, S.; Nummelin, A.; Hjalmarson, Å. Detection of interstellar ethylene oxide (c-C_2H_4O). *Astrophys. J.* **1997**, *489*, 753−757.

(8) Nummelin, A.; Dickens, J. E.; Bergman, P.; Hjalmarson, A.; Irvine, W. M.; Ikeda, M.; Ohishi, M. Abundances of ethylene oxide and acetaldehyde in hot molecular cloud cores. *Astron. Astrophys.* **1998**, *337*, 275−286.

(9) Ikeda, M.; Ohishi, M.; Nummelin, A.; Dickens, J. E.; Bergman, P.; Hjalmarson, A.; Irvine, W. M. Survey observations of c-C_2H_4O and CH_3CHO toward massive star-forming regions. *Astrophys. J.* **2001**, *560*, 792−805.

(10) Requena-Torres, M. A.; Martin-Pintado, J.; Martin, S.; Morris, M. R. The Galactic center: The largest oxygen-bearing organic molecule repository. *Astrophys. J.* **2008**, *672*, 352−60.

(11) Turner, B. E.; Apponi, A. J. Microwave detection of interstellar vinyl alcohol, CH_2CHOH. *Astrophys. J.* **2001**, *561*, L207−L210.

(12) Charnley, S. Acetaldehyde in star-forming regions. *Adv. Space Res.* **2004**, *33*, 23−30.

(13) Bennett, C. J.; Osamura, Y.; Lebar, M. D.; Kaiser, R. I. Laboratory studies on the formation of three C_2H_4O isomers − acetaldehyde (CH_3CHO), ethylene oxide (c-C_2H_4O), and vinyl alcohol (CH_2CHOH) − in interstellar and cometary ices. *Astrophys. J.* **2005**, *634*, 698−711.

(14) Hudson, R. L.; Moore, M. H. Solid-phase formation of interstellar vinyl alcohol. *Astrophys. J.* **2003**, *586*, L107−L110.

(15) Ward, M. D.; Price, S. D. Thermal reactions of oxygen atoms with alkenes at low temperatures on interstellar dust. *Astrophys. J.* **2011**, *741*, 121.

(16) Saito, S. Microwave spectroscopic detection of vinyl alcohol, CH_2═CHOH. *Chem. Phys. Lett.* **1976**, *42*, 399−402.

(17) Rodler, M.; Bauder, A. Structure of syn-vinyl alcohol determined by microwave spectroscopy. *J. Am. Chem. Soc.* **1984**, *106*, 4025−4028.

(18) Rodler, M. Microwave spectrum, dipole moment, and structure of anti-vinyl alcohol. *J. Mol. Spectrosc.* **1985**, *114*, 23−30.

(19) Hays, B. M.; Wehres, N.; DePrince, B. A.; Roy, A. A. M.; Laas, J. C.; Widicus Weaver, S. L. Rotational spectral studies of O(^{1}D) insertion reactions with methane and ethylene: Methanol and vinyl alcohol in a supersonic expansion. *Chem. Phys. Lett.* **2015**, *630*, 18−26.

(20) Bunn, H.; Soliday, R. M.; Sumner, I.; Raston, P. L. Far-infrared spectroscopic characterization of anti-vinyl alcohol. *Astrophys. J.* **2017**, *847*, 67.

(21) Melosso, M.; Melli, A.; Puzzarini, C.; Codella, C.; Spada, L.; Dore, L.; Degli Esposti, C.; Lefloch, B.; Bachiller, R.; Ceccarelli, C.; Cernicharo, J.; Barone, V. Laboratory measurements and astronomical search for cyanomethanimine. *Astron. Astrophys.* **2018**, *609*, A121.

(22) Melli, A.; Melosso, M.; Tasinato, N.; Bosi, G.; Spada, L.; Bloino, J.; Mendolicchio, M.; Dore, L.; Barone, V.; Puzzarini, C. Rotational and infrared spectroscopy of ethanimine: A route toward its astrophysical and planetary detection. *Astrophys. J.* **2018**, *855*, 123.

(23) Degli Esposti, C.; Dore, L.; Melosso, M.; Kobayashi, K.; Fujita, C.; Ozeki, H. Millimeter-wave and submillimeter-wave spectra of aminoacetonitrile in the three lowest vibrational excited states. *Astrophys. J., Suppl. Ser.* **2017**, *230*, 26.

(24) Kaushik, V. K. Centrifugal distortion effect in the microwave spectrum of vinyl alcohol. *Chem. Phys. Lett.* **1977**, *49*, 89−91.

(25) Rodler, M. Ph.D. Thesis, Eidgenössische Technische Hochschule (ETH) Zürich, Zürich, Switzerland, 1983.

(26) Müller, H. S.; Schlöder, F.; Stutzki, J.; Winnewisser, G. The Cologne Database for Molecular Spectroscopy, CDMS: A useful tool for astronomers and spectroscopists. *J. Mol. Struct.* **2005**, *742*, 215−227.

(27) Pickett, H. M. The fitting and prediction of vibration-rotation spectra with spin interactions. *J. Mol. Spectrosc.* **1991**, *148*, 371−377.

(28) Watson, J. K. G. Aspects of quartic and sextic centrifugal effects on rotational energy levels. In *Vibrational Spectra and Structure*; Durig, J., Ed.; Elsevier: Amsterdam, Netherlands, 1977; Vol. 6, pp 1−89.

(29) Lefloch, B.; et al. Astrochemical evolution along star formation: Overview of the IRAM Large Program ASAI. *Mon. Not. R. Astron. Soc.* **2018**, *477*, 4792−4809.

(30) Hollis, J. M.; Jewell, P. R.; Lovas, F. J.; Remijan, A. Green bank telescope observations of interstellar glycolaldehyde: Low-temperature sugar. *Astrophys. J.* **2004**, *613*, L45−L48.

(31) Higuchi, A. E.; Sakai, N.; Watanabe, Y.; López-Sepulcre, A.; Yoshida, K.; Oya, Y.; Imai, M.; Zhang, Y.; Ceccarelli, C.; Lefloch, B.; Codella, C.; Bachiller, R.; Hirota, T.; Sakai, T.; Yamamoto, S. Chemical survey toward young stellar objects in the perseus molecular cloud complex. *Astrophys. J., Suppl. Ser.* **2018**, *236*, 52.

(32) McGuire, B. A.; Carroll, P. B.; Dollhopf, N. M.; Crockett, N. R.; Corby, J. F.; Loomis, R. A.; Burkhardt, A. M.; Shingledecker, C.; Blake, G. A.; Remijan, A. J. CSO and CARMA observations of L1157. I. A deep search for hydroxylamine (NH_2OH). *Astrophys. J.* **2015**, *812*, 76.

(33) Araki, M.; Takano, S.; Sakai, N.; Yamamoto, S.; Oyama, T.; Kuze, N.; Tsukiyama, K. Long carbon chains in the warm carbon-chain-chemistry source L1527: First detection of C_7H in molecular clouds. *Astrophys. J.* **2017**, *847*, 51.

(34) Hily-Blant, P.; Faure, A.; Vastel, C.; Magalhaes, V.; Lefloch, B.; Bachiller, R. The nitrogen isotopic ratio of HC_3N towards the L1544 prestellar core. *Mon. Not. R. Astron. Soc.* **2018**, *480*, 1174−1186.

(35) McGuire, B. A.; Burkhardt, A. M.; Kalenskii, S. V.; Shingledecker, C. N.; Remijan, A. J.; Herbst, E.; McCarthy, M. C. Detection of the aromatic molecule benzonitrile (c-C_6H_5CN) in the interstellar medium. *Science* **2018**, *359*, 202−205.

(36) Cernicharo, J.; Lefloch, B.; Agúndez, M.; Bailleux, S.; Margulès, L.; Roueff, E.; Bachiller, R.; Marcelino, N.; Tercero, B.; Vastel, C.; Caux, E. Discovery of the ubiquitous cation NS^+ in space confirmed by laboratory spectroscopy. *Astrophys. J., Lett.* **2018**, *853*, L22.

(37) Jørgensen, J. K.; Schöier, F. L.; van Dishoeck, E. F. Physical structure and CO abundance of low-mass protostellar envelopes. *Astron. Astrophys.* **2002**, *389*, 908−930.

DOI: 10.1021/acsearthspacechem.9b00055
ACS Earth Space Chem. 2019, 3, 1189−1195

(38) Crapsi, A.; Caselli, P.; Walmsley, C. M.; Myers, P. C.; Tafalla, M.; Lee, C. W.; Bourke, T. L. Probing the evolutionary status of starless cores through N_2H^+ and N_2D^+ observations. *Astrophys. J.* **2005**, *619*, 379−406.
(39) Gratier, P.; Majumdar, L.; Ohishi, M.; Roueff, E.; Loison, J. C.; Hickson, K. M.; Wakelam, V. A new reference chemical composition for TMC-1. *Astrophys. J., Suppl. Ser.* **2016**, *225*, 25.
(40) Lis, D. C.; Goldsmith, P. F. Modeling of the continuum and molecular line emission from the sagittarius-B2 molecular cloud. *Astrophys. J.* **1990**, *356*, 195−210.
(41) Belloche, A.; Müller, H. S. P.; Menten, K. M.; Schilke, P.; Comito, C. Complex organic molecules in the interstellar medium: IRAM 30 m line survey of Sagittarius B2(N) and (M). *Astron. Astrophys.* **2013**, *559*, A47−187.
(42) Requena-Torres, M. A.; Martin-Pintado, J.; Rodríguez-Franco, A.; Martín, S.; Rodríguez-Fernández, N. J.; De Vicente, P. Organic molecules in the Galactic center. *Astron. Astrophys.* **2006**, *455*, 971−985.
(43) Burkhardt, A. M.; Dollhopf, N. M.; Corby, J. F.; Carroll, P. B.; Shingledecker, C. N.; Loomis, R. A.; Booth, S. T.; Blake, G. A.; Herbst, E.; Remijan, A. J.; McGuire, B. A. CSO and CARMA observations of L1157. II. Chemical complexity in the shocked outflow. *Astrophys. J.* **2016**, *827*, 21.

DOI: 10.1021/acsearthspacechem.9b00055
ACS Earth Space Chem. 2019, 3, 1189−1195